PHYSICS CLUB
OCTOBER STEM SCHOOL

COMPASS

Comparative Analysis of the 2D Ising Model Utilizing Local Update and Cluster Algorithms

Faissel Mokhaimer, Nada Walid

February 8, 2026

STEM October Physics Club, COMPASS Computational Physics Program

Abstract

The two-dimensional square-lattice ferromagnetic Ising model is a tool incorporated in understanding phase transition and ferromagnets behavior across different temperatures. This paper explores the Ising model at low temperature and near the critical temperature, where algorithms get computationally expensive, utilizing local update, Metropolis and Heat Bath, and cluster, Wolff and Swendsen–Wang, algorithms. This paper analyzes key thermodynamic observables, magnetization, energy, susceptibility, heat capacity, and Binder cumulants, across different lattice sizes and at different temperatures to estimate computational cost, characterize the phase transition, and finite-size effects. Results show that local update algorithms suffer from critical slowing down near the critical temperature ($T_c \approx 2.269$), leading to long integrated autocorrelation time and higher peaks in thermodynamic quantities. However, cluster algorithms reduce this effect significantly by updating correlated spin clusters, resulting in shorter autocorrelation times and improved sampling near critical temperature. Nevertheless, both local update and cluster algorithms become inefficient at low temperatures as a result of low acceptance rates in local update algorithms and inefficient growth of clusters in cluster algorithms. This study highlights the advantages of cluster algorithms for simulating the 2D square-lattice Ising model near T_c and the inefficiency of both algorithm types at low temperatures.

Keywords: N-body Simulation; Barnes-Hut; Particle-Mesh; Time Complexity Optimization

1 Introduction

The 2D Ising model on a square lattice is a paradigmatic system in statistical mechanics, showing a continuous phase transition between an ordered ferromagnetic state at low temperature and a disordered paramagnetic state above the critical temperature $T_c \approx 2.269$. While the model is solvable by exact mathematics in the thermodynamic limit, Monte Carlo simulations remain essential for studying finite-size effects, dynamic properties, and as in this project the comparative performance of modern sampling algorithms.

Near T_c, conventional local update methods such as the Metropolis and heat bath algorithms suffer from critical slowing down, where the autocorrelation time diverges with system size. This makes obtaining statistically independent samples computationally prohibitive. Cluster-update techniques most notably the Wolff single cluster and Swendsen Wang multi cluster algorithms were developed specifically to overcome this limitation. By flipping entire clusters of spins that are strongly linked in a single move, they dramatically suppress critical slowing down and provide efficient sampling in the critical region. Further sampling enhancements can be achieved through parallel tempering, which accelerates tunneling between temporarily stable states by allowing replicas at different temperatures to exchange configurations.

In this study, five distinct Monte Carlo strategies for the 2D Ising model are implemented, tested, and compared, which are: the local update Metropolis and heat bath algorithms, the cluster update Wolff and Swendsen–Wang methods, and the advanced multi temperature parallel tempering technique. Key equilibrium observables are measured:

magnetization, energy, susceptibility, specific heat, and the Binder cumulant across a temperature range spanning the phase transition. More importantly, algorithmic efficiency is quantified through integrated autocorrelation times and the CPU time required per independent sample. The results offer a clear, practical guide for choosing an appropriate sampling algorithm depending on the temperature range and system size, with implications for the simulation of more complex spin systems and lattice models.

2 Methodology

2.1 The Ising Model

The paper discusses the two-dimensional ferromagnetic Ising model on a square lattice, defined by the Hamiltonian (Eq. 2.1)

$$H = -J \sum_{\langle i,j \rangle} s_i s_j \tag{2.1}$$

The spin variable at site i takes values $s_i = \pm 1$, and the coupling constant $J > 0$ favors ferromagnetic alignment. The summation $\langle i, j \rangle$ runs over all nearest neighbor pairs.

Furthermore, it adopts natural units by setting $J = 1, k_B = 1$, for computational convenience. So, temperature T is expressed in units of J/k_B and the inverse temperature is $\beta = 1/T$.

Additionally, it simulates an $L \times L$ lattice with periodic boundary conditions in both directions, removing edge effects and approximating the thermodynamic limit essential for studying bulk thermodynamics and finite size scaling.

The model shows a well-known second-order phase transition at the Onsager critical temperature (Eq. 2.2)

$$T_c = \frac{2}{\ln(1 + \sqrt{2})} \approx 2.269. \tag{2.2}$$

When $T < T_c$, the system develops self-generated magnetization and long-range ferromagnetic order, but when $T > T_c$, it remains in a disordered paramagnetic phase.

2.2 Monte Carlo Algorithms

The paper implements and compares Monte Carlo algorithms. Each method employs a distinct spin update mechanism, leading to differences in computational efficiency.

Metropolis Algorithm

The Metropolis algorithm uses a random-based accept–reject procedure. In each update:

- A random spin s_i is chosen.
- The sum of its four nearest neighbors on the 2D lattice (with periodic boundaries) is computed.
- The energy changes when the spin that was flipped is (Eq. 2.3):

$$\Delta E = 2J s_i \sum_{\text{neighbors}} s_{\text{neighbor}} \tag{2.3}$$

The flip is accepted with probability (Eq. 2.4)

$$P_{\text{acc}} = \min(1, e^{-\Delta E/T}). \tag{2.4}$$

If rejected, the spin remains unchanged. One Monte Carlo sweep = L^2 attempts (one per spin on average).

Heat Bath Algorithm

In contrast to Metropolis, the heat bath (Gibbs sampler) algorithm directly draws a spin from its local equilibrium distribution. For a chosen spin s_i:

- The local field $h_i = \sum_{\text{neighbors}} s_j$ is computed.
- The spin is set to $+1$ with probability (Eq. 2.5)

$$P_+ = \frac{1}{1 + e^{-2\beta J h_i}} \tag{2.5}$$

The spin is set to -1 with probability (Eq. 2.6)

$$1 - P_+ = \frac{1}{1 + e^{+2\beta J h_i}} \tag{2.6}$$

Each update independently draws s_i from $\{+1, -1\}$ with these probabilities.

Wolff Single Cluster Algorithm

To overcome critical slowing down near T_c, the Wolff algorithm builds and flips a connected cluster of aligned spins:

- A random site is selected as the cluster seed.
- Neighboring spins of the same orientation are added with probability (Eq. 2.7)

$$p_{\text{add}} = 1 - e^{-2\beta J}. \tag{2.7}$$

Step 2 repeats recursively for all newly added spins. The entire cluster is flipped.

One MCS corresponds to one cluster update. The mean cluster size diverges near T_c, enabling efficient sampling in the critical region.

Swendsen–Wang Multi Cluster Algorithm

The Swendsen–Wang algorithm updates the entire lattice at once via a multi cluster approach:

- Bond activation: Between each pair of neighboring like spins, a bond is activated with probability $p_{\text{add}} = 1 - e^{-2\beta J}$.
- Cluster identification: Connected components of activated bonds define independent spin clusters.
- Cluster flipping: Each cluster is flipped independently with probability $1/2$.

This global update rapidly decorrelates configurations, particularly near criticality.

2.3 Measured Observables

Thermodynamic properties are extracted from Monte Carlo time series. Unless noted otherwise, all quantities are reported per spin.

Magnetization

The primary order parameter is the magnetization per spin (Eq. 2.8):

$$m = \frac{1}{N} \sum_{i=1}^{N} s_i \tag{2.8}$$

where $N = L^2$. Below T_c, the Z_2 symmetry of the Hamiltonian is spontaneously broken. To avoid cancellation between degenerate ordered states in finite simulations, the model also computes the absolute magnetization (Eq. 2.9):

$$|m| = \frac{1}{N} \left| \sum_{i=1}^{N} s_i \right|. \tag{2.9}$$

Energy

The internal energy per spin is $e = H/N$. The total energy H is computed directly from the Hamiltonian. For efficiency on a periodic square lattice, the model implements (Eq. 2.10):

$$H = -J \sum_{i,j} \left[s_{i,j} s_{i+1,j} + s_{i,j} s_{i,j+1} \right], \tag{2.10}$$

where indices wrap periodically.

Susceptibility and Specific Heat

From magnetization and energy fluctuations, the magnetic susceptibility χ (Eq. 2.11) and specific heat C (Eq. 2.12) is derived via fluctuation dissipation relations:

$$\chi = \frac{N}{T} \left(\langle m^2 \rangle - \langle |m| \rangle^2 \right) \tag{2.11}$$

$$C = \frac{N}{T^2} \left(\langle e^2 \rangle - \langle e \rangle^2 \right). \tag{2.12}$$

Binder Cumulant

The fourth-order Binder cumulant (Eq. 2.13)

$$U_L = 1 - \frac{\langle m^4 \rangle}{3 \langle m^2 \rangle^2} \tag{2.13}$$

is used to locate T_c through finite-size scaling. Near criticality, $U_L(T)$ becomes approximately independent of L, crossing points for different L yield a precise estimate of T_c.

Autocorrelation Analysis

Algorithmic efficiency is quantified via autocorrelation. For an observable A, the normalized autocorrelation function is (Eq. 2.14)

$$C_A(t) = \frac{\langle A(k)A(k+t)\rangle - \langle A\rangle^2}{\langle A^2\rangle - \langle A\rangle^2}, \tag{2.14}$$

where t is the lag in Monte Carlo steps. The integrated autocorrelation time is estimated as (Eq. 2.15)

$$\tau_{\text{int}} = \frac{1}{2} + \sum_{t=1}^{t_{\max}} C_A(t), \tag{2.15}$$

with $t_{\max} > 6\tau_{\text{int}}$ to ensure convergence. The effective number of independent samples is then (Eq. 2.16)

$$N_{\text{indep}} = \frac{N_{\text{meas}}}{2\tau_{\text{int}}}. \tag{2.16}$$

Algorithmic Performance Metric

To compare raw efficiency, the CPU time per independent sample is defined (Eq. 2.17):

$$t_{\text{indep}} = \tau_{\text{int}} \times t_{\text{sweep}}, \tag{2.17}$$

where t_{sweep} is the wall clock time for one Monte Carlo sweep. Minimizing t_{indep} is the practical objective when choosing an algorithm for production runs.

2.4 Simulation Protocol

A consistent and reproducible protocol is applied across all algorithms to ensure a fair comparison. Simulations are conducted over a matrix of system sizes L and temperatures T, following the steps outlined below.

System Parameters

The paper examines square lattices with linear sizes $L \in \{16, 32, 64, 128\}$. Temperatures are sampled in the range $T \in [1.5, 3.5]$ with a coarse resolution $\Delta T = 0.05$ away from T_c. In the critical region near the Onsager temperature $T_c \approx 2.269$, the grid is refined to $\Delta T = 0.01$. All simulations use $J = 1$ and periodic boundary conditions.

Initialization and Thermalization

The initial spin configuration is chosen to expedite equilibration:

- For $T > T_c$: a random disordered configuration (spins ± 1 with equal probability).
- For $T < T_c$: a fully magnetized state (all spins up).

All simulations were implemented in Python using NumPy arrays. For fair comparison, simulations at each (L, T) pair were initialized with identical random seeds and spin configurations. For reproducibility, a fixed random seed was used for each parameter set, with variations introduced via seed offsets for independent trials. The Wolff and Swendsen–Wang algorithms used a stack-based breadth first search for cluster identification.

3 Results

In this section, the numerical results of Monte Carlo simulations were presented. Several algorithms of the two-dimensional Ising model were incorporated in the project, which were the Metropolis, heatbath, Wolff cluster, and Swendsen–Wang algorithms. Simulations were performed on square lattices of sizes $L = 16, 32, 64$, and 128. The temperature values studied were $T = 0.21, 0.61, 1.01, 1.41, 1.81, 2.11, 2.21, 2.23, 2.25, 2.26, 2.269, 2.27, 2.29, 2.31, 2.33, 2.35, 2.41, 2.81, 3.21, 3.61, 4.01, 4.41$. Temperatures were chosen to be finely spaced near the critical temperature ($T_c = 2.269185$) and more coarsely spaced away from it. The measured observables are the average magnetization, total energy, magnetic susceptibility, heat capacity, Binder cumulant crossings, integrated autocorrelation time, and CPU time per independent sample. Thermodynamic quantities are presented primarily for the reference system size $L = 32$, while integrated autocorrelation times were analyzed across multiple system sizes.

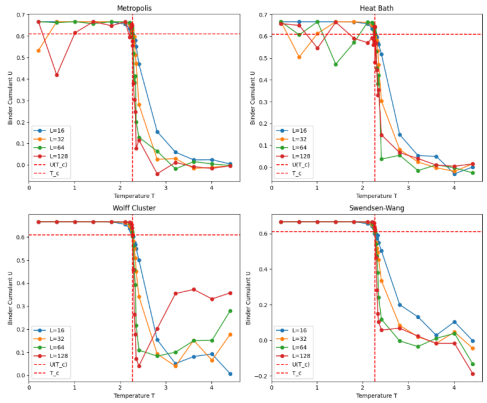

Figure 1: Binder Cumulant Crossings

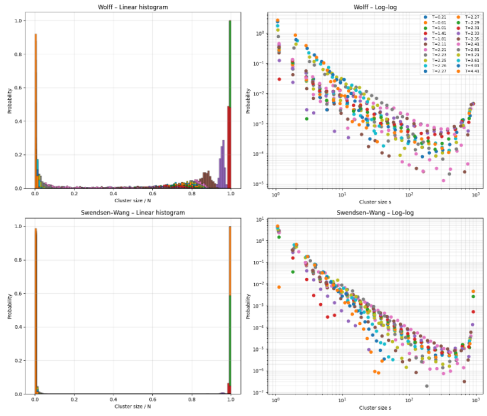

Figure 2: Cluster Sizes and Distributions

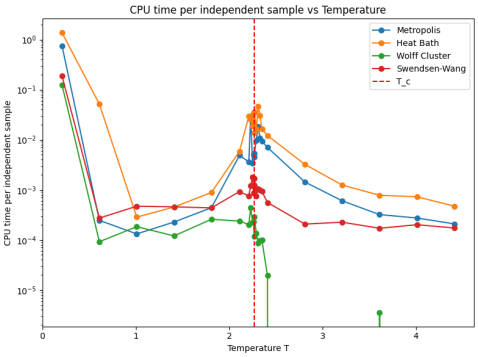

Figure 3: CPU time per independent Sample vs Temperature

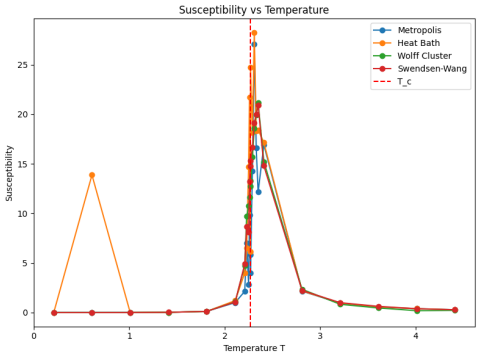

Figure 7: Susceptibility vs Temperature

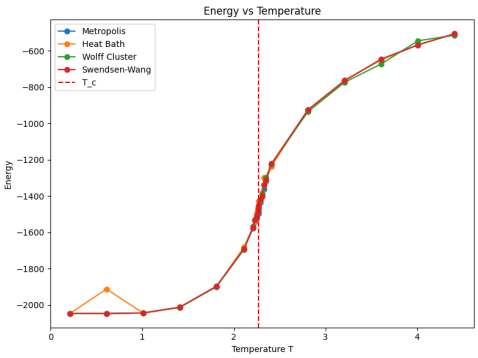

Figure 4: Energy vs Temperature

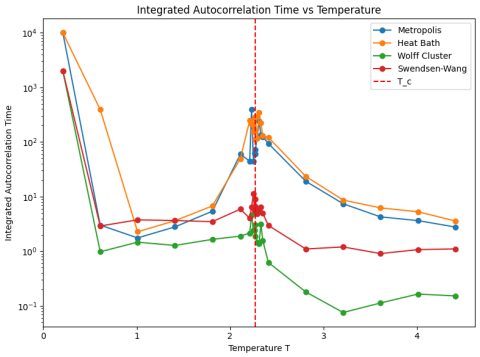

Figure 8: Integrated Autocorrelation Time vs Temperature

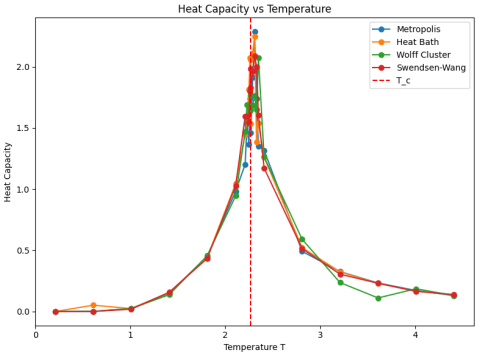

Figure 5: Heat Capacity vs Temperature

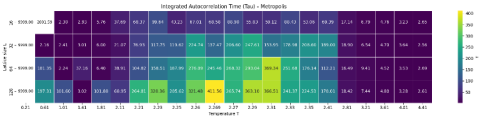

Figure 9: Integrated Autocorrelation Time – Metropolis Heatmap

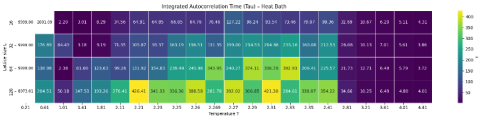

Figure 10: Integrated Autocorrelation Time – Heat Bath Heatmap

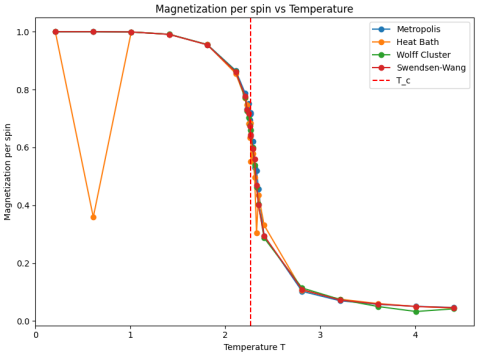

Figure 6: Magnetization per spin vs Temperature

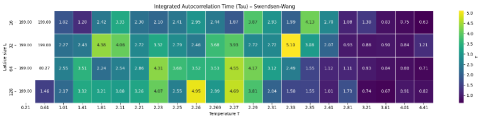

Figure 11: Integrated Autocorrelation Time – Swendsen-Wang Heatmap

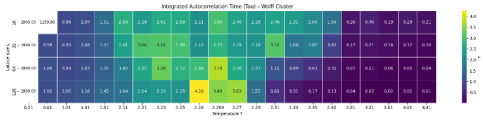

Figure 12: Integrated Autocorrelation Time – Wolff Cluster Heatmap

4 Discussion

4.1 Critical Behavior from magnetization and susceptibility

The behavior of magnetization and susceptibility together provide evidence for the transition phase. The rapid decrease of magnetization with increasing temperature is accompanied by a peak in susceptibility, which reflects the growth of fluctuations near criticality. The location of susceptibility maximum is consistent with the temperature range where magnetization changes most rapidly, confirming the identification of the criticality region. As the lattice size increases, the susceptibility peak becomes sharper and more pronounced, indicating better fluctuations near T. Additionally, Metropolis and Heat Bath have higher peaks as they suffer from critical slowing down. This is particularly evident in the Heat Bath magnetization at low temperatures, which does not fully reach equilibrium. However, cluster algorithms like Swendsen–Wang and Wolff Cluster efficiently do spin updates, reducing autocorrelation and producing a lower, and smoother susceptibility peaks.

4.2 Energy and Heat Capacity near The Transition

The energy shows a smooth dependence on temperature for all algorithms, while the heat capacity shows a clear maximum in the critical region. This peak of heat capacity demonstrated increased energy fluctuations as the system approaches the transition phase. With increasing lattice size, the heat-capacity peak becomes higher and narrower, highlighting the influence of critical correlations. Local update algorithms, Metropolis and Heat Bath, have higher peaks in heat capacity as they suffer from critical slowing down. This can be observed in Heat Bath energy at low temperatures, where the 2D Ising model doesn't reach equilibrium. However, cluster algorithms efficiently do spin updates, having smoother heat capacity peaks. Finally, the temperature where heat capacity reaches its maximum agrees with the critical region from magnetization and susceptibility, proving internal consistency of the measured observables.

4.3 Binder Cumulants and Finite-size Scaling

Binder cumulant crossings for different lattice sizes provide an estimate of the critical temperature (T_c = 2.269), which proves that critical temperature is size-independent. The convergence of binder cumulant crossings increases as the lattice size increases, indicating finite-size effects. Small shifts in the crossing temperatures can be attributed to finite-size effects and statistical uncertainties. Still, binder cumulant crossings offer a more precise determination of the transition point T_c than peak-based methods (susceptibility and heat capacity).

4.4 Autocorrelation Times and Critical Slowing Down

Integrated autocorrelation time shows strong dependence on temperature and system size. For local update algorithms, the autocorrelation time increases sharply near the critical temperature and grows rapidly with lattice size, demonstrating critical slowing down. On the other hand, cluster algorithms reduce this effect significantly by updating correlated clusters of spins, leading to much shorter autocorrelation time in the critical region. Heatmaps of integrated autocorrelation time across different temperatures and lattice sizes clearly show this contrast, with local update algorithms exhibiting a broad region of high integrated autocorrelation times in the critical region, while cluster methods maintain weak size dependence, effectively eliminating critical slowing down.

4.5 Computational Efficiency and CPU time per independent sample

The differences in autocorrelation function and integrated autocorrelation times directly impact computational cost and CPU time per independent sample. Although cluster algorithms evidently require more computation per Monte Carlo update, their reduced integrated autocorrelation times lead to lower CPU time per independent sample near criticality. In contrast, local update algorithms become severely inefficient in the critical region, especially as lattice size increases, despite their lower per computational step cost. Away from the transition phase (critical region), where autocorrelation times are high, local update algorithms remain competent, highlighting the pros and cons of update cost and sampling efficiency.

4.6 Implications for algorithms

While all algorithms accurately produce equilibrium thermodynamic quantities, their performance differ significantly in terms of integrated autocorrelation times and CPU time per independent sample specifically in the critical region. Cluster algorithms are better for studying critical region behavior and large lattice sizes, whereas local update algorithms remain competitive away from criticality. These results demonstrate the importance of combining equilibrium observables with computational metrics when assessing Monte Carlo algorithms and studying statistical physics phenomena like the 2D Ising model.

5 Conclusion

To conclude, the study successfully simulated the 2D square-lattice Ising model across various system sizes L = 16, 32, 64, 128, to analyze the efficiency of local update algorithms, Metropolis and Heat Bath, and cluster algorithms, Wolff and Swendsen-Wang, at low temperatures and near the critical temperature (Tc = 2.269). The study shows phase transition in the critical region characterized by high peaks in susceptibility and heat capacity, while magnetization smoothly descends and energy increases as temperature increases.

Moreover, the study demonstrates the algorithms' trade-offs, facing critical slowing down, where integrated autocorrelation

times and CPU time per independent sample increase significantly near Tc, which are severe in local update algorithms.

However, cluster algorithms work efficiently near Tc, reducing integrated autocorrelation times and CPU time per independent sample. Still, at low temperature, the four algorithms exhibit reduced efficiency, producing higher integrated autocorrelation times and CPU time per independent sample because of low spin acceptance rates in local update algorithms and inefficient cluster growth in Wolff and Swendsen-Wang algorithms.

Further studies of the Ising model could extend to analyzing other algorithms, such as parallel tempering, alongside increasing lattice sizes, temperature range, and computational budget to reveal more about the behavior at low temperatures, critical temperature, and high temperature with a broader and deeper perspective.